Experimental and Numerical Analysis of the Influence of Thermal Control on Adsorption and Desorption Processes in Adsorbed Natural Gas Storage

D. Ybyraiymkul[1*], KC. Ng[2], A. Kaltayev[1]

[1]Al-Farabi Kazakh National University, Almaty, Kazakhstan
[2]King Abdullah University of Science and Technology, Water Desalination and Reuse Center, Jeddah, Saudi Arabia

Article info

Received:
10 October 2015

Received in revised form:
22 December 2015

Accepted:
5 February 2016

Abstract

Natural gas,the most environmentally friendly fossil fuel, can be stored in a vessel based on adsorption technology, designed for energy efficient storage of natural gas at relatively medium pressures (3–4 MPa).The application of adsorption technology will reduce the energy consumption for gas compressing or gas liquefying compared to compressed and liquefied natural gas storage methods,also, it will lead to cost savings in compressing and cooling equipment. While charging/discharging of adsorbed natural gas (ANG) vessel, the latent heat of adsorption counteracts to adsorption/desorption process, as the result, thermal effect causes a reduction of vessel capacity. Therefore,the influence of thermal control on adsorption and desorption processes in adsorbed natural gas vessel was studied experimentally and numerically in this paper. The study focusing on the three dimensional heat exchange is important in order to understand the heat transfer phenomena and analyze influence of thermal control comprehensively. The temperature and adsorption uptake profiles in the vessel were demonstrated in the numerical simulation. Comparison of experimental and simulation results showed that deviation between experimental and numerical results was 0.1%.

Nomenclature

ρ_g – gas density;
$\vec{u}_g$ – gas velocity;
ε_t – total porosity;
ε_b – bed porosity;
ε_p – particle porosity;
ρ_s – solid adsorbent density;
a – adsorption uptake or amount of adsorbed gas per unit mass of adsorbent;
P – gas pressure;
μ_g – dynamic viscosity of gas;
E – gas activation energy;
R – gas constant;
T – temperature;
K_S – mass transfer coefficient,
a_{eg} – amount of adsorbed gas at equilibrium pressure and temperature,
W_0 – maximum volumetric adsorption equilibrium uptake;
v_a – adsorbed phase specific volume;
n – heterogeneity parameter;
P_{cr} – critical pressure;
T_{cr} – critical temperature;
$c_{p,g}$ – gas heat capacity;
$c_{p,a}$ – adsorbed gas heat capacity;
$c_{p,s}$ – solid adsorbent heat capacity;
H_a – heat of adsorption;
k – heat conductivity;
d_l – thickness of fins;
ρ_l – density of fin;
k_l – conductivity of fin;
c_l – heat capacity of fin.

1. Introduction

Cost-effectiveness and environmental safety of the use of natural gas as a fuel for motor vehicles are obvious, as it is accompanied by a reduction in carbon monoxide (CO) emissions by 40%, carbon dioxide (CO_2) – by 25%, nitrogen oxide (NO_x) – by 10% and smog-forming volatile organic compounds by 92% [1]. Also, natural gas could be produced in abundant amount from associated petroleum gas or from coal seams, and it is mainly composed of methane (95%). Methane is a fuel with the lowest combustion emissions compared to

* Corresponding author. E-mail: doskhan@bk.ru

other hydrocarbon fuels. However, the problem of storing natural gas leads to the restriction of its consumption. Methane at standard temperature cannot be changed into liquid state only by compression, because of its critical temperature (-82.59 °C) [2]. Under standard conditions methane is very inappropriate for motor vehicles as a fuel mainly due to low volumetric energy density which is 0.038 MJ/l and it is only 0.12% of gasoline. The usage of conventional gas storing methods as compressed natural gas (CNG) storage is constrained by expensive compressing equipment and by hazards associated with high pressure (25 MPa) [1–2]. The application of liquefied natural gas (LNG) method-limited by costly equipment for liquefaction and by the possibility of hazards related to low temperature (-163 °C). In addition, LNG method requires trained personnel who can assess and control hazard in refueling operations.

Another way of storing methane is using adsorbent materials inside storage tanks where during charging process methane molecules can be attracted onto surface of pores of adsorbents by means of Van der Waals forces that change the phase of the gas close to liquid [1–5, 11–15]. At the same time, the pressure inside the tank is at reasonable safe range which is about 3–4 MPa. Therefore, adsorbed natural gas technology seems more cost effective than others, as fueling/refueling process is consuming less energy, and there is no need for expensive compression tools. During charging of vessels, thermal energy is generated due to exothermic adsorption process and bed temperature is increased, thus reducing adsorption capacity of porous material [2]. On the other hand, discharging is the opposite of the charging process, where during desorption,bed temperature decreases and it leads to lowering of the amount delivered gas. During fueling and refueling of the storage tank, gas storage and delivery capacities lose 25%, compared to capacities that are obtained in case of ideal isothermal process [2, 11, 15]. Hence, control of the thermal energy in the storage tank is responsible for desirable adsorption/desorption of methane into/from porous material.

One-dimensional (radial) and 2D axisymmetric transient models for the charge/discharge process of adsorbed methane cylinders have been studied by several authors [2, 5–7]. In some models [5], the thermal regulation was not considered while in others [10, 12] a storage vessel was cooled/heated with U-shaped heat exchange pipe. More recently, the effect of heating the outside of the ANG cylinder with exhaust gas was evaluated [7].

In present work, the heat transfer in ANG vessel was studied experimentally and numerically. The main objective is to analyze three dimensional heat transfer as the heat exchanger device is composed of flat fins and array of tubes. Additionally, in-plane heat flux equation is used in for modeling heat exchange in flat fins.

2. Experimental setup

Experimental prototype of ANG storage vessel was installed as shown in Fig. 1. It is composed of stainless steel cylinder (316 SSL), finned tube heat exchanger mounted inside of the vessel which is filled with adsorbent (Maxsorb III).

The prototype is also composed of charging/discharging installation, apparatus designed to circulate water though tubes of the heat exchanger where temperature of the water is controlled by thermostat, the data acquisition system which consists of a laptop with the program written in LabView, and data logger (Agilent 34970A) for real-time data acquisition. Temperature sensors are placed into the vessel for measuring temperature of heat exchanger tubes, fins, gas and adsorbent. Moreover, devices such as pressure regulators, water flow meter, gas flow controller, pressure sensors, valves and other necessary devices are used to conduct the experiment. A vacuum pump is connected to the cylinder for extraction of residual gas from adsorbent. In order to prepare the sample ANG storage vessel for the experiment, following steps are required. First, ANG vessel should be evacuated with vacuum pump for about 24 h. At the step of evacuating the vessel, water is circulated through the heat exchanger tubes with a temperature close to 80 °C (353.15 K) to accelerate desorption of the residual gas from the adsorbent. Lastly, the vessel is filled up with methane until the inside pressure reaches 0.1 MPa and cooled down to 25 °C (298.15 K) to reach initial conditions. The purity grade of the sample used was 99.95% of CH_4 (methane).

2.1. Charging and discharging procedure

1) In the beginning of each run, pressure and temperature in the vessel were examined for consistency with initial conditions;

2) There after, when the temperature became uniform inside the vessel, the pressure regulator of the methane cylinder was adjusted to 3.0 MPa;

3) The vessel inlet valve was opened and the change in time of some variables (such as pressure, temperature and etc.) was registered;

4) When the temperature became stable and homogeneous throughout the vessel, the valve of the gas cylinder was closed. After that, the flow of

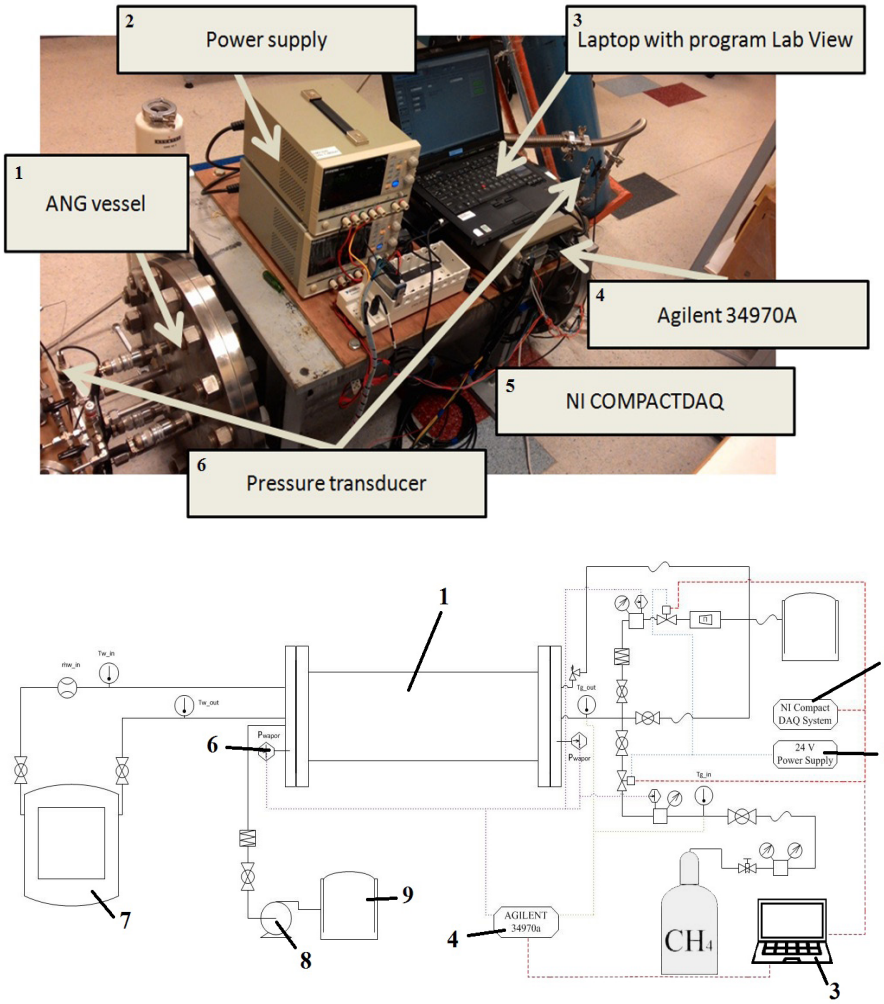

Fig. 1. Experimental prototype and schematic diagram of ANG storage vessel: 1 – ANG vessel; 2 – power supply; 3 – laptop; 4 – Agilent 34970A; 5 – NI COMPACTDAQ; 6 – pressure transducer; 7 – thermostat; 8 – vacuum pump; 9 – fume hood.

gas was diverted to the fume hood using the mass flow controller, thereby unloading the gas from the ANG vessel, while recording the change of monitored variables;

5) At the stage when the charge and discharge procedures were finished, reports with recorded experimental data were obtained with the purpose of comparing them to simulated results.

The temperature field of the storage vessel was measured by thermistors located at different sites of the adsorbent bed. The mass flow controller was used to control and determine the amount of discharged methane.

3. Mathematical Model

3.1. Governing equations

Methane is a primary component of natural gas (more than 95%), so its properties are studied in this work. Mathematical model of ANG vessel based on mass, energy, momentum conservation equations and linear driving force (LDF) model. The main assumptions are listed below:

1) The adsorbed and the gas phases are in instantaneous equilibrium condition within the porous media, as the adsorption process is governed by first order kinetics, which is physically consistent.

2) The temperature of the adsorbent and gas in elementary volume of porous media is the same due to a high intensity heat transfer between solid and gas phases.

3) The adsorbed phase is incompressible, as the behavior of adsorbed gas is close to liquid condition.

4) Temperature of tubes is assumed constant and equal to initial temperature, because inlet water temperature fluctuation is almost zero and velocity of water in tubes is as high as 1 m/s.

Mass conservation equation is derived by spatial averaging technique,

$$\frac{\partial \rho_g}{\partial t} + \nabla(\rho_g \vec{u}_g) = -\frac{\rho_s(1-\varepsilon_t)}{\varepsilon_b}\frac{\partial a}{\partial t} \qquad (1)$$

The last term of Eq. (1) is the mass flux due to the adsorption/desorption. The gas motion inside of the porous medium is described by spatially averaged Navier-Stokes equations with the additional term which represents resistance of the porous medium,

$$\rho_g \frac{\partial \vec{u}_g}{\partial t} + \rho_g (\vec{u}_g \cdot \nabla)\vec{u}_g = -\nabla P + \mu_g \nabla^2 \vec{u}_g - \left(\frac{\mu_g}{K} \varepsilon_b \vec{u}_g + Kf |\vec{u}_g| \vec{u}_g \right) \quad (2)$$

Kf and *K* can be determined from the Ergun equation. Density of methane is calculated from Van der Waals equation. The adsorption process, which occurs because of the strength of intermolecular interactions at the interface between the adsorbent and gas, is described by linear driving force model:

$$\frac{\partial a}{\partial t} = (a_{eq} - a) K_S \exp\left(-\frac{E}{RT} \right) \quad (3)$$

where α_{eq} is calculated by Dubinin-Astakhov equation:

$$a_{eq} = \frac{W_0}{v_a} \exp\left\{ -\left[\frac{RT}{E} \ln\left(\frac{P_{cr}}{P} \left(\frac{T}{T_{cr}} \right)^2 \right) \right]^n \right\} \quad (4)$$

Adsorption isotherm and adsorption kinetics parameters for MaxsorbIII/Methane were obtained from literature [8, 9]. The energy balance for ANG vessel can be written as:

$$\left(\varepsilon_b \rho_g c_{p,g} + \rho_p c_{p,a} a + \rho_p c_{p,s} a \right) \frac{\partial T}{\partial t} + \varepsilon_b \rho_g c_{p,g} \vec{u}_g \cdot \nabla T = \nabla \cdot (k \nabla T) + \rho_p H_a \frac{\partial a}{\partial t} \quad (5)$$

where $k = \varepsilon_b k_g + (1 - \varepsilon_t) k_s$ is heat conductivity. The last term in Eq. (5) is heat generation due to adsorption/desorption of gas.

In order to describe heat transfer in fins, the heat equation is used that describes the in-plane heat flux in the layer:

$$d_l \rho_l c_l \frac{\partial T}{\partial t} + \nabla_l \cdot (-d_l k_l \nabla T) = -q_l$$

where q_l is the net out flux of heat through the top and bottom faces of the layer and ∇_l indicates the "nabla" operator projected onto plane of highly conductive layer.

3.2. Boundary and initial conditions

Computational domains, boundary conditions and heat exchanger construction are presented in Fig. 2, and the size being similar to the actual dimensions. Inlet pressure and inlet temperature are the same as in the experiment. Parameters from Eq. (2), *Kf* and *(1/K)* are equal to zero at gas domain. Initial conditions are also same as in the experiment:

P = 1.1 MPa, T = 25.5 °C, $\vec{u}_g = 0$, (for charging)

P = 3.0 MPa, T = 25.2 °C , $\vec{u}_g = 0$, (for discharging).

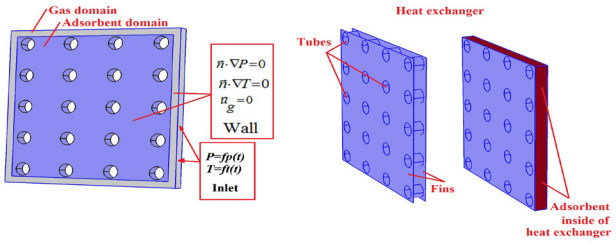

Fig. 2. Boundary conditions and computational domains.

4. Result and discussion

4.1. Comparison analysis for adsorption

Adsorption and desorption processes in ANG vessel were simulated, as the numerical results allow comprehensively describing and analyzing of the entire mechanism of heat and mass transfer. Experimental study is essential to validate results obtained by simulation. On the basis of the mathematical model of ANG vessel, numerical results were established using the finite element method based software COMSOL Multiphysics. Computational domain was discretized using a high quality mesh, element size was lower than 2 mm. Figure 3 indicates the adsorption uptake and temperature contours in the middle cross section (between fins) of the computation domain (Fig. 2).

According to the simulation results, the high temperature region is located at the central region of the cross-section, because of rectangular tube layout, where the vertical and horizontal distances between tubes are different. Conductive heat transfer dominates convection heat transfer as Peclet number is equal to 0.3 and it is lower than 1. As shown in Fig. 4a, averaged temperature profile of the adsorbent layer is raised to 304.95 K at the beginning of the charging. However, the temperature reaches 299.15 K after short period (595 sec), since the adsorbent layer have been cooled with the heat exchanger while charging of ANG vessel.

Figure 4e shows pressure profile of ANG vessel, where the slope has almost linear behavior at the beginning of charging process. However, time required to achieve charging pressure, is longer, because of significantly decreasing of mass flow rate, which is proportional to charging and ANG vessel pressure difference. In the adiabatic case, temperature of adsorbent increases to 348.75 K (Fig. 4b) and maximum adsorption uptake reaches 0.125 (Fig. 4d), which is also include initial uptake. Amount of filled gas in adiabatic condition is almost twice (1.96) lower than in thermal regulated condition (Fig. 4c).

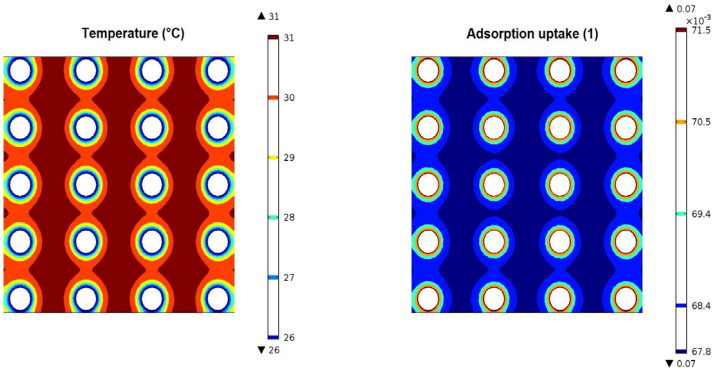

Fig. 3. Temperature and adsorption uptake contours at t = 140 sec

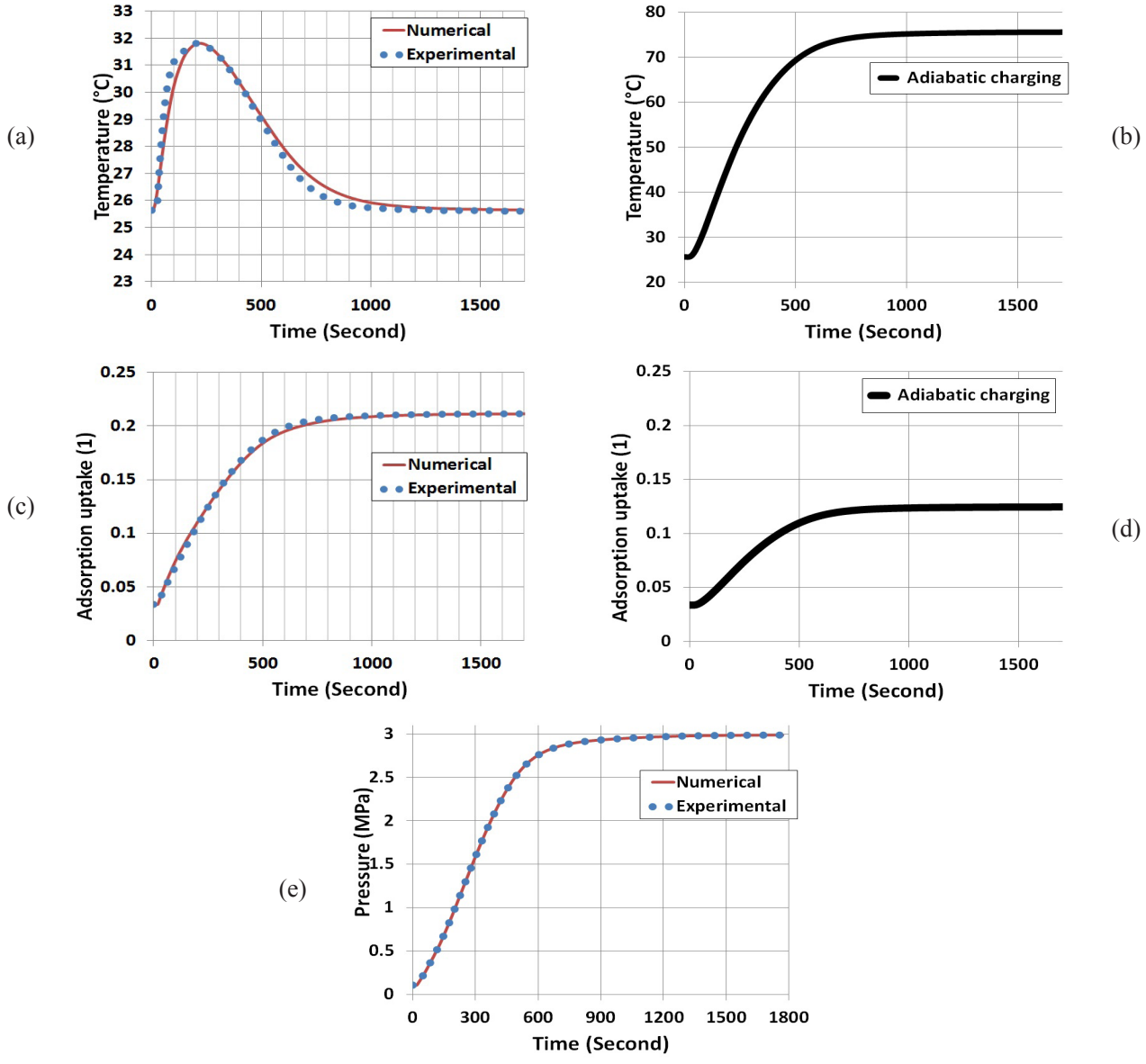

Fig. 4. Temperature (a, b), adsorption uptake (c, d) and pressure (e) profiles.

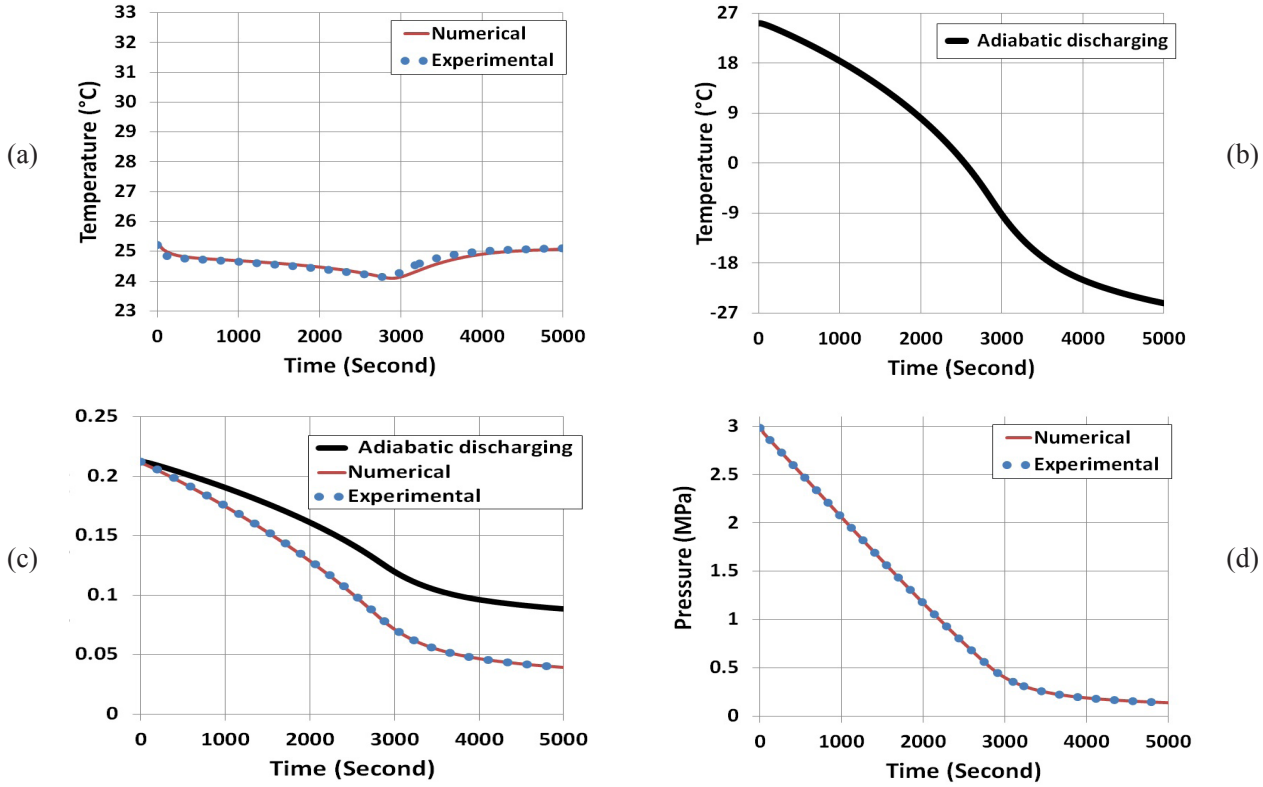

Fig. 5. Temperature (a, b), adsorption uptake (c) and pressure (d) profiles.

4.2. Comparison analysis for desorption

The main problem of discharging of ANG storage is the temperature drop during desorption, which lowers the performance below feasible in the case without thermal control. In order to remain temperature constant there was used heat exchange device as described previously. Averaged temperature, adsorption uptake and pressure profiles are shown in Fig. 5. The numerical and experimental results (Fig. 5a) exhibit that the adsorbent layer temperature fluctuation is very small (about 1.1 K). Compared with the adiabatic case (Fig. 5b), results show close to isothermal conditions. Adsorption uptake varies from 0.212 to 0.037, and amount of desorbed gas is 28% higher than in adiabatic case (Fig. 5c). In adiabatic case, the temperature of the adsorbent layer falls from 298.35 K to 247.85 K, which is very large deviation.

The adsorbent loses its ability to desorb a gas at low temperatures, which is lead to decreasing of the amount of desorbed gas, compared to the isothermal case. Figure 5d shows the change in pressure in 5000 sec, where pressure is reduced from 3.0 MPa to 0.13 MPa. Temperature and adsorption uptake contours are shown in Fig. 6. Contours are displayed in the middle cross-section (between fins) of the heat exchanger during the discharging. The result shows that temperature contour is nearly homogenous, as the central region deviated from initial temperature only for -1 K.

The major heat transfer takes place from both the fins and tubes. Peclet number is equal to 0.05 and it is important to observe that conduction heat transfer dominates significantly while discharging of ANG vessel. So, the simulation model represents adequately heat transfer in adsorbent layer and heat exchanger, where used extended surfaces (fins) and tubes. During the calculation there was used "fully coupled" algorithm and the "PARDISO" solver. Also, there was performed a mesh refinement study until the solution was mesh independent.

5. Conclusion

The investigations of thermal control effect on adsorption and desorption processes in adsorbed natural gas storage were carried out in the experiment and numerical simulation. The temperature distribution of the adsorbent layer was evaluated using a set of thermistors during the charging/discharging process. Also, the mathematical model heat and mass transfer is developed and described in detail, which take into account the effect of adsorption on the thermodynamic state of the whole system. Besides, heat transfer in ANG vessel was clearly demonstrated in the 3D numerical simulation. The results show that the high temperature

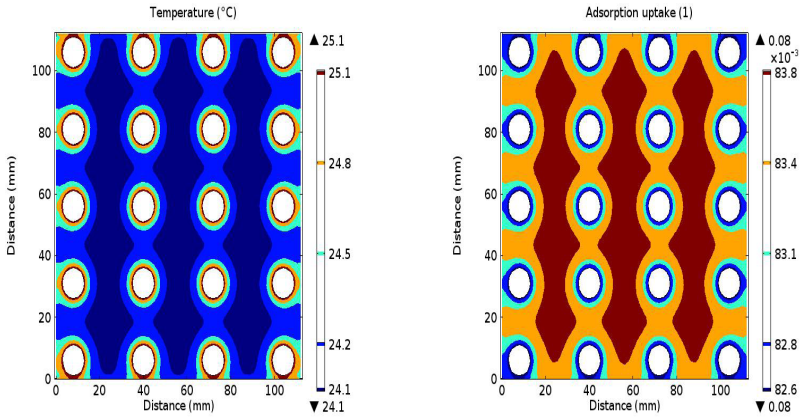

Fig. 6. Temperature and adsorption uptakecontours at t = 2910 s.

region is located at the central region of the computational domain at the beginning of charging process, but after short period of time temperature was cooled down to initial temperature. So, the higher adsorption uptake value was achieved while using of fined and tubed heat exchanger during charging of vessel. While the discharging of ANG vessel there was found that adsorbent layer temperature was close to isothermal condition. Also, during discharging, residual amount of gas was decreased for 28%, compared to adiabatic case. Moreover, domination of conduction heat transfer was demonstrated in the numerical simulation for both charging and discharging case.

Results show the effectiveness of the heat exchanging device. Both experiment and simulation showed a satisfactory agreement for the temperature and pressure for adsorbent layer. Deviation between experimental and simulation results was 0.1%. Thus, these results are useful for further improvement of thermal regimes of charging/discharging which will lead to reduction of residual amount of gas left at depletion pressure.

Acknowledgments

The authors gratefully acknowledge the financial support given by grants (GF3-1566) from Ministry of Education and Science of the Republic of Kazakhstan, and from National University of Singapore.

References

[1]. D. Lozano-Castello, J. Monge-Alcaniz, M.A. Casa-Lillo, D. Cazorla-Amoros, Fuel 81 (14) (2002) 1777–1803.
[2]. J.C. Santos, J.M. Gurgel, F. Marcondes, Appl. Therm. Eng. 90 (5) (2015) 258–265.
[3]. M. Beckner, A. Dailly, Appl. Energ. 149 (2015) 69–74.
[4]. A. Saez, M. Toledo, Appl. Therm. Eng. 29 (13) (2009) 2617-2623.
[5]. S.C. Hirata, P. Couto, L.G. Lara, R.M. Cotta, Int. J. Therm. Sci. 48(6) (2009) 1176–1183.
[6]. R. Basumatary, P. Dutta, M. Prasad, K. Srinivasan, Carbon 43 (3) (2005) 541–549.
[7]. P.K. Sahoo, B.P. Prajwal, S. K. Dasetty, M. John, B.L. Newalkar, N.V. Choudary, K.G. Ayappa, Appl. Energ. 119 (2014) 190–203.
[8]. K.A. Rahman, W.S. Loh, H. Yanagi, A. Chakraborty, B.B. Saha, W.G. Chun, K.C. Ng, J. Chem. Eng. Data 55 (11) (2010) 4961–4967.
[9]. W.S. Loh, K.A. Rahman, A. Chakraborty, B.B. Saha, Y.S. Choo, B.C. Khoo, K.C. Ng, J. Chem. Eng. Data 55 (8) (2010) 2840–2847.
[10]. K.A. Rahman, W.S. Loh, A. Chakraborty, B.B. Saha, W.G. Chun, K.C. Ng, Appl. Therm. Eng. 31 (10) (2011) 1630–1639.
[11]. Y. Sun, C. Liu, W. Su, Y. Zhou, L. Zhou, Adsorption 15 (2) (2009) 133–137.
[12]. X.D. Yang, Q.R. Zheng, A.Z. Gu, X.S. Lu, Appl. Therm. Eng. 25 (4) (2005) 591–601.
[13]. S.H. Yeon, S. Osswald, Y. Gogots, J.P. Singer, J.M. Simmons, J.E. Fischer, M.A. Lillo-Ródenas, A. Linares-Solano, J. Power Sources 191 (2) (2009) 560–567.
[14]. R.B. Rios, M. Bastos-Neto, M.R. Amora Jr., A.E.B. Torres, D.C.S. Azevedo, C.L. Cavalcante Jr., Fuel 90 (1) (2011) 113–119.
[15]. F.N. Ridha, R.M. Yunus, M. Rashid, A.F. Ismail, Appl. Therm. Eng. 27 (1) (2007) 55–62.